Citation: Yalin Zhu, Yanke Gao, Liming Wu, et al. Experimental study of cumulative plastic strain in reinforced sand under cyclic loading. *Journal of Harbin Institute of Technology (New Series)*. DOI:10.11916/j.issn.1005-9113.2024041

Experimental Study of Cumulative Plastic Strain in Reinforced Sand Under Cyclic Loading

Yalin Zhu[1,2], *Yanke Gao*[1], *Liming Wu*[1], *Qian Xu*[1*] *and Juxiang Chen*[1,2]

(*1. School of Civil and Hydraulic Engineering, Hefei University of Technology, Hefei 230009, Anhui, China;*
2. Key Laboratory of Civil Engineering Structure and Materials, Hefei 230009, Anhui, China)

Abstract: Long-term cyclic train loading can cause settlement and deformation of the roadbed, affecting the normal operation of trains. In order to investigate the strain pattern of reinforced sandy soil under train loading, a series of dynamic triaxial tests were carried out using multi-stage loading, focusing on the effects of the number of reinforcement layers, the confining pressure and the mesh size of the geogrid on the accumulated plastic strain of reinforced sandy soil. Moreover, prediction models were proposed. The test results show that: 1) The cumulative plastic strain versus vibration times of the specimens under different reinforcement layers exhibited three stages, namely, the rapid development stage, the rate transformation stage and the stability stage; 2) The cumulative plastic strain decreases with increasing the number of reinforcement layers, but the magnitude of the effect of reinforcement on the cumulative plastic strain decreases with increasing the number of reinforcement layers, increasing the perimeter pressure and decreasing the mesh size of the geogrid have similar effects on the cumulative plastic strain pattern as increasing the number of reinforcement layers; 3) Combined with the cumulative plastic strain law, a comprehensive model is proposed and the coefficient of determination is greater than 0.99. Furthermore, The cumulative plastic strain evolution law can be effectively predicted. The significance of parameters A, B and C is analyzed in detail. This study can provide theoretical references for further understanding of the deformation characteristics and settlement prediction of railway subgrade.

Keywords: reinforced sand; dynamic triaxial test; accumulated plastic strain; predictive model.

CLC number: TU4 **Document code**: A **Article ID**: 1005-9113(2025)00-0000-10

0 Introduction

Under the action of train load for a long time, the railway subgrade will have settlement deformation, which will lead to the decline of track smoothness and stability, and even cause certain safety risks to the operation of the train. Reinforced soil structure is widely used in subgrade strengthening engineering because of its good engineering economy, construction convenience and seismic performance. With the rapid development of railway in China, the traditional study on roadbed engineering cannot meet the actual demand, especially for the reinforcement and deformation need to further study.

Domestic and foreign scholars have carried out extensive research on the deformation characteristics of roadbed under cyclic load. Wichtmann et al.[1] mainly studied the cumulative strain law of sand with high cycle times and small strain amplitude. Nguyen et al.[2] studied the strain accumulation phenomenon of coarse-grained soil under high frequency and low amplitude loads through dynamic triaxial tests, and analyzed it from macroscopic and microscopic perspectives. Huang et al.[3] found that the development of cumulative deformation is uncertain when undrained, however, the cumulative deformation quickly reaches stability when drained. Huang et al.[4] found that the cumulative axial strain increment of soft clay decreases with increasing cyclic confining pressure under different test conditions.

Received 2024-04-29.

Sponsored by the National Natural Science Foundation of China (Grant No.42077249), and the Innovation an Entrepreneurship Training Program for College Students of Hefei University of Technology (Grant No. S202410359131, Grant No. X202410359244).

* Corresponding author: Q. Xu. MSc. Email: 1316186314@qq.com.

Wang et al.[5] studied the effects of the number of reinforced layers and confining pressure on the axial cumulative strain of reinforced gravel soil, and further analyzed the development mechanism of cumulative strain. Song et al.[6] carried out a large-scale dynamic triaxial test of geogrid-reinforced sand and found that at the initial loading stage, the cumulative deformation of both plain sand and cellular soil was small, while the amplitude of dynamic load was large, the cumulative plastic deformation of cellular soil was significantly reduced compared with that of plain soil. Cui et al.[7] obtained that the cumulative axial strain of the soil after reinforcement will decrease through a series of cyclic triaxial tests, and the more the number of reinforcement layers, the smaller the cumulative axial strain.

Cumulative plastic deformation model is the theoretical basis for solving the deformation characteristics and settlement problems of roadbed under long-term cyclic load. There are three main models for predicting the development trend of cumulative plastic strain, which respectively are Monismith model (Exponential model)[8], semi-logarithmic model[9] and hyperbolic model[10]. respectively, The Monismith model (Exponential model) is easy to apply but may not be accurate at high cycle times. The semi-logarithmic model is suitable for the initial growth phase, but may have limitations in the long term. The hyperbolic model can better simulate the saturation stage of cumulative plastic deformation, meanwhile, a lot of experimental data is needed to determine the model parameters. Given the limitations of these models, many researchers have improved them. Based on the exponential model, Li et al.[11] and Chai et al.[12] took into account factors such as deviational stress and static strength, and achieved good prediction results. Gao et al.[13] proposed an improved Monismith model with more ideal results. The larger the dynamic stress amplitude, the more loading times are required for the specimen deformation stability. Wang[14] analyzed the relationship model between cumulative plastic deformation and loading times, dynamic stress level, static breaking strength and other parameters. Liu et al.[15] divided the cumulative deformation of gravel with different water content gradations like decay type and destruction type, and found that the destruction type could be predicted by an exponential model. Li et al.[16] reinforced the construction waste soil and found that the cumulative deformation conforms to the hyperbolic model within 10 cycles, and the modified exponential model after 10 cycles. These studies show that, in practice, many factors need to be considered, such as the type of soil, the properties of the reinforced material, the type of reinforcement and the cyclic loading characteristics. To select or construct the cumulative plastic deformation model that is most appropriate for specific engineering conditions.

With the rapid development of the transport industry, the dynamic characteristics of the soil under train load have attracted considerable attention. The deformation and settlement of unreinforced sandy soil under the action of train load is large, which endangers the safety and service life of the track. In practical engineering applications, reinforcement technology can effectively improve the strength and stability of the soil. However, there are different opinions on the study of the dynamic characteristics of reinforced soils. In particular, the study of the dynamic characteristics of reinforced sand under multi-stage cyclic loading is inadequate.

In order to make up for this lack of research, a dynamic triaxial test of reinforced sand has been carried out in this paper. The cumulative plastic strain curves under different reinforcement layers, confining pressures and geogrid mesh sizes are fully considered. Based on the previous prediction model, a comprehensive model is proposed to predict the cumulative plastic strain of reinforced soil, and the significance of the relevant parameters in the model is also analyzed. The research results can provide a theoretical basis for the improvement of the design and construction of reinforced soil. It has important engineering application value for improving the stability and durability of railway subgrade.

1 Test Equipment and Test Content

1.1 Test Equipment

The instrument used in the test is the GDS saturated soil dynamic triaxial instrument (as shown in Fig.1) produced by the European and American Dadi Science and Technology Group. The instrument is composed of pressure chamber, drive motor, confining and counter-pressure controller, load sensor, pore pressure sensor, GDSLAB data acquisition and control program and other modules. The key technical indicators of the dynamic triaxial

instrument are: frequency range 0.01 Hz-5 Hz, maximum axial load 10 kN, maximum confining pressure 2000 kPa, displacement accuracy 0.07%, axial force accuracy 1N.

Fig.1 Physical drawing of GDS saturated soil moving triaxis

1.2 Test Soil Sample and Preparation

The sample of soil test was taken from Hefei local river sand. The particle analysis test showed that the non-uniformity coefficient Cu = 2.6 and curvature coefficient Cc = 1.2. The sand was poorly graded sand, and the particle grading curve is shown in Fig.2. The relative density of the sand sample is 2.66, the maximum dry density is 1.65g/cm^3, and the minimum dry density is 1.40 g/cm^3. The controlled dry density of the sample is 1.57 g/cm^3, and its relative density is 0.72, which means the sand is classified as dense.

Thesizeofthesampleis39.1 mm×80 mm.However, in the actual project, the size of geogrid mesh is relatively large. In order to reduce the impact of size effect, the fiber-glass mesh cloth is selected as the stiffening material to replace the geogrid. The two types of stiffening materials with mesh sizes are named geogrid A and geogrid B, respectively.

The geogrids used in the test are depicted in Fig. 3, and the technical parameters of the geogrid are listed in Table 1.

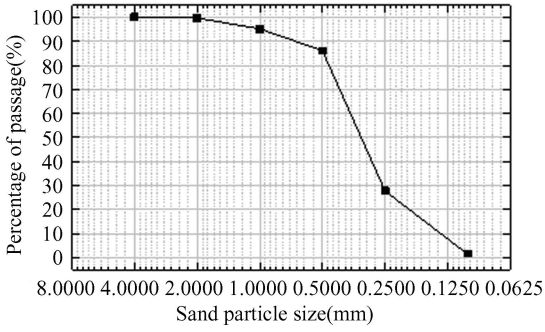

Fig.2 Particle grading curve of sand soil

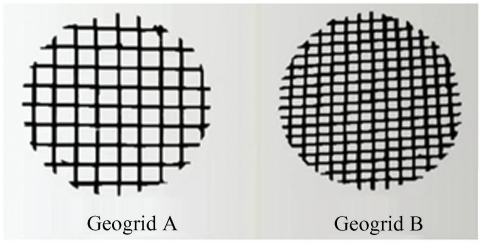

Fig.3 Geogrids used in the test

Table 1 Technical parameters of geogrid

Material name	Material	Mesh size(mm)	Breaking elongation (%)		Break strength (kN/m)	
			radial direction	cross direction	radial direction	cross direction
Geogrid A	Fiber-glass	3×3	2.6	2.5	30	25
Geogrid B	Fiber-glass	2.0×2.5	2.6	2.5	30	25

According to the requirements of the degree of compaction in the Technical Specifications for Highway Subgrade Construction (JTG D30-2015). The sample preparation process in this paper is as follows: 1) The sand is dried before the test. 2) A certain mass of packing is put into the test cylinder of the dynamic triaxial instrument, and the sample is prepared by the stratified vibration method. It is divided into four layers, each layer of sand quality is the same, and the control is 38 g. 3) After the sand has solidified to the required height, the surface is shaved. After each layer of packing is vibrated and compacted, the geogrid is laid according to the requirements of the scheme. 4) After the sample preparation is completed, a back pressure of -10 kPa is applied to the sample via GDSLAB to prevent the sample from being damaged by disturbance.

The diameter of the geogrid used in this test is slightly smaller than that of the sample, primarily to avoid interaction between the geogrid and the sample boundary[16], and secondly to prevent the geogrid from cutting the rubber film.

1.3 Testing Scheme

The waveforms used in dynamic triaxial test are

generally sine wave and half sine wave. In order to simulate train load, half sine wave was chosen to simulate train load in this test[3]. Combined with the actual acting frequency of train load, the test loading frequency of half sine wave was set to 1 Hz. In order to consider the influence of confining pressure on the mechanical properties of reinforced sand, confining pressure of 50 kPa, 75 kPa, 100 kPa was taken to simulate the confining pressure of different depth roadbed[17]. The schematic diagram of reinforced geogrid is shown in Fig.4.

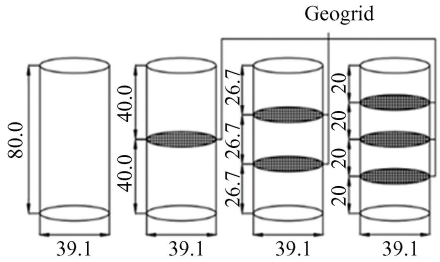

Fig.4 Schematic diagram of geogrid reinforcement (unit / mm)

With reference to Erlingsson[18], Tang[19] and other relevant literature, it can be considered that the dynamic strain generated by loading the sample 3000 times under a small dynamic stress amplitude is equivalent to loading a small number of vibrations under a large dynamic stress amplitude. For train loads with long duration and small amplitude, the dynamic stress amplitudes of the first, second and third stage cyclic loads are set as 50 kPa, 150 kPa and 250 kPa by referring to the train load values in the code for design of railway subgrade[20] and combining with the multi-stage dynamic triaxial test scheme of Ma et al.[21]. The failure standard of the test is that the cumulative plastic strain reaches 5%, and the vibration times of each stage of cyclic load is tentatively set at 3000 times. If the failure standard is not reached, the test ends when the frequency of cyclic loads reaches 9000 times. The multi-stage cyclic loading waveform is shown in Fig. 5. The specific test conditions are listed in Table 2.

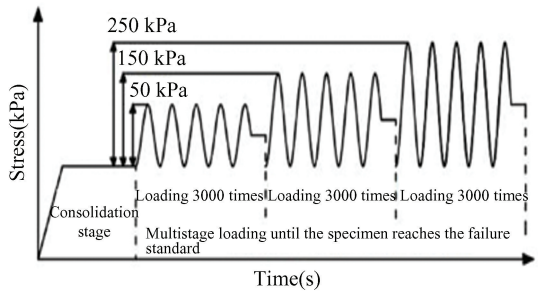

Fig.5 Multilevel semi-sine wave loading waveform

Table 2 Classification of test conditions

Test condition	Confining pressure(kPa)	Dynamic stress amplitude(kPa)	Reinforcement layers
1	50	50/150/250	unreinforced
2	75	50/150/250	unreinforced
3	100	50/150/250	unreinforced
4	50	50/150/250	one layer reinforced A
5	50	50/150/250	two layers reinforced A
6	50	50/150/250	three layers reinforced A
7	50	50/150/250	three layers reinforced B

1.4 Test Process

The test process under each working condition is basically similar, which can be divided into five steps: 1) Prepare the sand sample by layers to ensure that the sample has the same density. 2) After filling the pressure chamber with water, 20kPa protective confining pressure is applied to the sample. 3) For sample saturation, the combined saturation method of CO_2 saturation followed by water head saturation and finally reverse pressure saturation was adopted. When the B value is equal to or above 95%, saturation is considered to be complete. 4) The consolidation is carried out by isotropic consolidation with consolidation ratio Kc = 1. When the reverse pressure volume remains unchanged, the consolidation is considered to be complete. 5) Multistage half-sinusoidal cyclic loads are applied. The test data is generated automatically in the GDSLAB data acquisition system.

2 Test Results Analysis

In this paper, three influential factors are considered, which are reinforcement layers, confining pressure and geogrid mesh size. The undrained dynamic triaxial test of consolidated sand is carried out. Because the cumulative plastic strain curve of the sample under multiple cyclic loads is too dense, in order to observe its law, the cumulative plastic strain

curve with vibration times is plotted separately.

2.1 Cumulative Plastic Strain Development Law

2.1.1 *Influence of the number of reinforcement layers on the cumulative plastic strain*

The cumulative plastic strain ε_d of the sample under different number of reinforced layers, the relation curve with vibration N is shown in Fig.6. It can be clearly seen from Fig.6(a) that the relation curve with N and ε_d presents three stages. The first stage (the number of vibrations ranges from 0 to 500 times) is the rapid development stage of cumulative plastic strain value, mainly because the sample begins to receive dynamic load, the internal pores of the sand will be quickly compacted, and the cumulative plastic strain is more obvious. The cumulative plastic strain at this stage accounts for the vast majority of the total cumulative plastic strain. The second stage is the transformation stage from large to small cumulative plastic strain rate. At this stage, a new skeleton structure has been formed inside the sand, and the influence of dynamic stress on the sand gradually becomes smaller. The third stage is the stable stage, when the dynamic stress on the sample becomes fatigue, the cumulative plastic strain increases at a slow and steady rate.

With the increase of the number of reinforced layers, the cumulative plastic strain of the sample gradually decreases, and the slope of the N and ε_d curve also gradually decreases. In the three layers reinforced sample, the slope of the curve is close to a horizontal line, indicating that reinforcement can effectively improve the stiffness of the sample and reduce the settlement deformation of the sandy soil subgrade. The effect coefficient of reinforcement R_{ε_d} [22] was introduced to evaluate the degree of influence of reinforcement on the cumulative plastic strain of sand, which shows as follows:

$$R_{\varepsilon_d} = \frac{\varepsilon_{d0} - \varepsilon_{di}}{\varepsilon_{d0}} \tag{1}$$

R_{ε_d} is the cumulative plastic strain reinforcement effect coefficient; $\varepsilon_{d0} - \varepsilon_{di}$ is the final difference of cumulative plastic strain between layer i and unreinforced layer; ε_{d0} is the final strain value of cumulative plastic strain when unreinforced.

In Fig.6(a), as the number of reinforced layers increases, R_{ε_d} are 0.334, 0.483, 0.566, respectively, the reinforcement effect is getting better and better. However, as the number of reinforced layers increases, the increment of R_{ε_d} is 0.334, 0.149 and 0.083 respectively, showing a decreasing trend. It shows that the effect of reinforcement on cumulative plastic strain gradually decreases. This is consistent with the research results of Wang et al.[5] on reinforced gravel soil. Combining the indirect influence zone theory[23], as the number of reinforced layers increases, the influence areas of the indirect influence zone will superimpose each other, and the reinforcement effect will be affected. It is shown that the effect of reinforcement on cumulative plastic strain gradually decreases as the number of reinforced layers increases.

It can be seen from Fig.6(b) and (c) that when unreinforced sand sample σ_d = 150 kPa, the failure standard of 5% is reached first. The one layer and two layers reinforced sample reach the failure standard when σ_d = 250 kPa, and only the three layers reinforced sample still do not reach the failure standard at the end of the test. This also shows that reinforcement can effectively reduce the cumulative plastic strain of sand, and the cumulative plastic strain decreases with the increase of reinforcement layers.

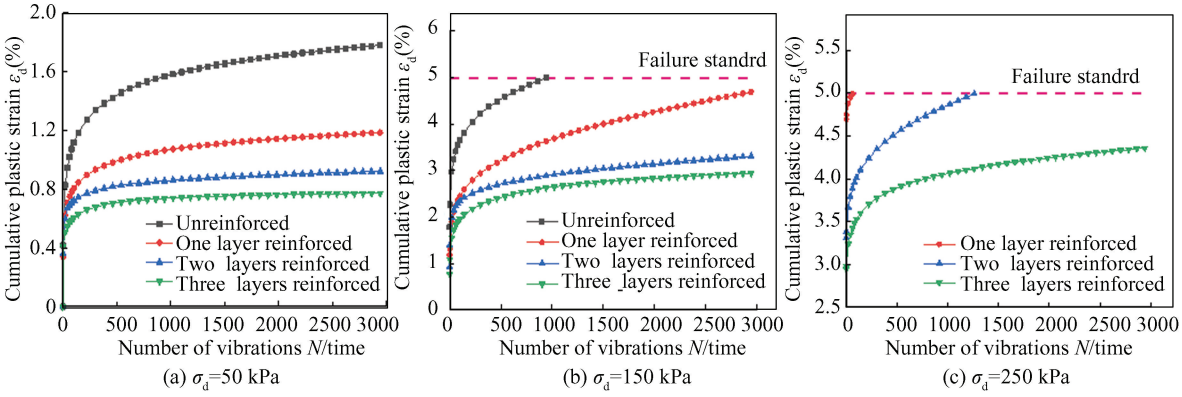

Fig.6 Relationship curves ε_d and N for different reinforced layers

2.1.2 *Influence of confining pressure on the cumulative plastic strain*

The relationship between cumulative plastic strain ε_d and vibration number N of the sample under different confining pressures is shown in Fig. 7. The changing law of N and ε_d under different confining pressures is similar to that under different reinforcement layers. It can be seen from Fig. 7 (a) that under the three confining pressures, the maximum cumulative plastic strain is 1.877%, 0.85% and 0.349%, respectively. It can be seen that the confining pressure has a great influence on the cumulative plastic strain, since increasing the confining pressure can significantly reduce the cumulative plastic strain of the sample. As can be seen from Fig. 7 (b) and (c), when σ_3 = 50 kPa, the sample first reaches the failure standard under the second cyclic load. When σ_3 = 75 kPa, the sample reached the failure standard under the third cyclic load. When σ_3 = 100 kPa, the sample did not reach the failure standard. The reason is that, with a constant consolidation ratio, as the confining pressure rises, the density of the sand also rises. This is because the pores between the sand particles of the sample have been compressed during consolidation. When the cyclic load is applied, the cumulative plastic strain is smaller.

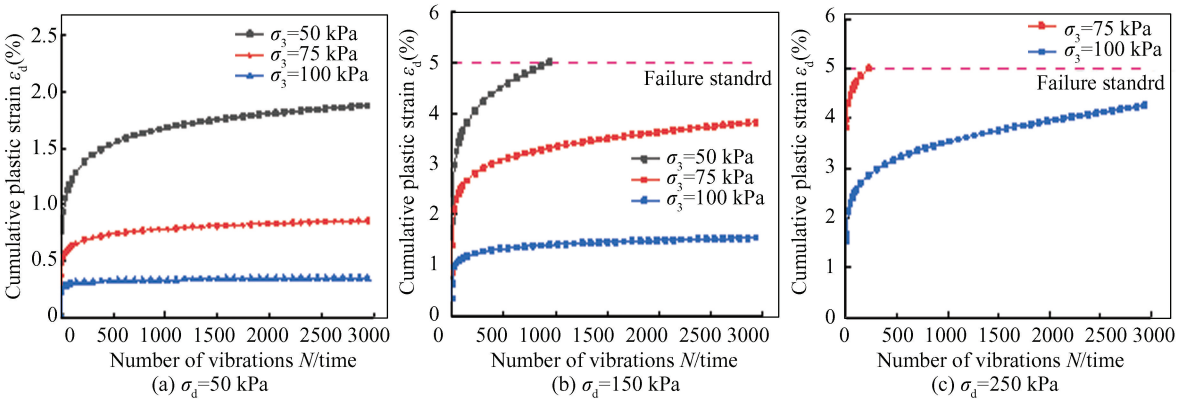

Fig.7 Relationship curves ε_d and N under different confining pressure

2.1.3 *Influence of different geogrids on the cumulative plastic strain*

The relationship between cumulative plastic strain ε_d and vibration N of the samples with different geogrids reinforcement is shown in Fig. 8. It can be seen that when the mesh size of the geogrids decreases, the deformation resistance of the reinforced sand samples under various cyclic loads is further strengthened, which is mainly reflected in the reduction of cumulative plastic strain. Moreover, the cumulative plastic strain varies under the influence of three dynamic stress amplitudes, which are 0.099%, 0.427% and 0.541%, respectively. It can be seen that with the increase of dynamic stress amplitude, the cumulative plastic strain difference between two sides becomes more and more obvious, and the high dynamic stress amplitude can better reflect the reinforcement effect caused by the reduction of mesh size. Reducing the mesh size of the geogrid, results in a greater number of grille ribs, which increases the friction resistance between the reinforced soil. When the interaction is stronger, a larger normal stress is required to achieve the same level of cumulative plastic strain. In the dynamic triaxial test, the cumulative plastic strain decreases as the mesh size decreases.

Comparing Fig. 8 (a), (b) and (c), as the dynamic stress amplitude increases, the slope of the relationship curve between ε_d and N also increases. Under the effect of small dynamic stress amplitude, the soil remains stable at the later stage of vibration and the cumulative plastic strain changes little. However, under the effect of large dynamic stress, the cumulative plastic strain still increases at a certain rate in the late period of vibration. It shows that the structure of the soil will be affected and the settlement amount of the soil will increase greatly when the dynamic stress is large.

2.2 Cumulative Plastic Strain Prediction Model

2.2.1 *Proposal of prediction model*

In recent years, many scholars have studied the cumulative plastic strain prediction model of soil mass. The most commonly used empirical model is the Monismith model. In practice, after a certain cyclic load, the strain of the railway subgrade tends to

be stable, resulting in a relatively constant deformation. In contrast, the cumulative plastic strain of the Monismith model continues to increase as the vibration times increases. Therefore, the development trend of Monismith model is inconsistent with that of stability curve, and there are certain defects[24]. Another commonly used empirical model is hyperbolic equation. However, after comparative analysis of Ref. [25], it is found that although hyperbolic model can well fit the final development trend of stable curve, it cannot predict the cumulative plastic strain value at small vibration times, because the cumulative plastic strain of hyperbolic model almost reaches the final strain value at the beginning of vibration. The development process of cumulative plastic strain is missing, which is inconsistent with the actual test law. In summary, on the basis of the experimental data, after comparing and analyzing the Monismith model and the hyperbolic model, this paper proposes a comprehensive model that combines the advantages of the two models, as shown in Eq.(2).

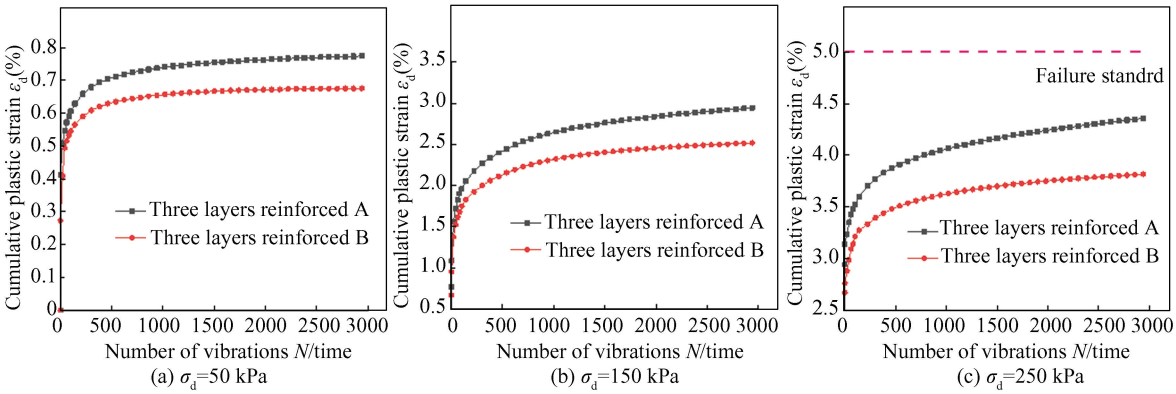

Fig.8 Relationship curve between ε_d and N under different geogrid reinforcement

$$\varepsilon_P = \frac{AN^B}{C + N^B} \tag{2}$$

where, ε_P is the cumulative plastic strain, N is the number of cyclic loads, and A, B and C are the model parameters.

Below, Monismith model, hyperbolic model and comprehensive model are used to fit the test data. The fitting effects of the three empirical models are shown in Fig. 9 (Taking the cumulative plastic strain of reinforced sand under different reinforcement layers as an example). As can be seen from the Fig.9, for the cumulative plastic strain of unreinforced sand and reinforced sand, the hyperbolic model has the worst fitting effect, and its overall trend is relatively gentle, which is not applicable to sand with large cumulative plastic strain changes. The Monismith model has a relatively good fitting effect, and the coefficient of determination R^2 is higer than 0.97. The comprehensive model has the highest fitting degree and the determination coefficient R^2 is higer than 0.99, which can better predict the cumulative plastic strain of unreinforced sand and reinforced sand. The hyperbolic model in Fig.9(c) had poor fitting effect and was not drawn.

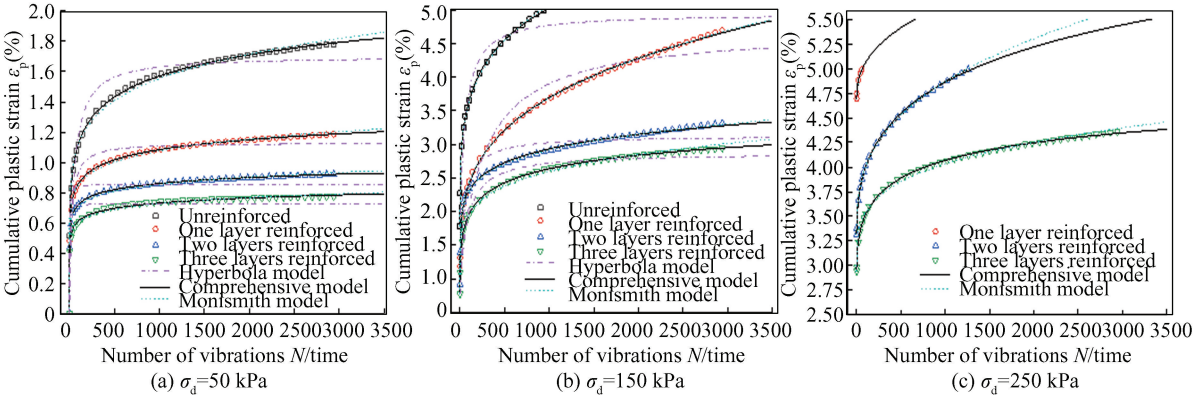

Fig.9 Fitting effect of three empirical models

2.2.2 Fitting parameter analysis

Fig.10 shows the influence curve of model parameters on cumulative plastic strain. According to Fig.10(a), when parameters B and C are determined, model parameter A mainly affects the maximum cumulative plastic strain in the ε_P -N curve, the results show that the number of reinforced layers, confining pressure and mesh size of geogrids have the greatest influence on the maximum cumulative plastic strain. Therefore, it is possible to establish a good relationship between the number of reinforced layers, confining pressure, mesh size of geogrids and vibration frequency in order to better analyze the relationship between the parameters. It can be seen from Fig.10(b) that when parameters A and C are determined, model parameter B mainly affects the slope of the ε_P -N curve, which increases with the increase of the value of parameter B. No matter how the value of B changes, its initial cumulative plastic strain value and final cumulative plastic strain value remain unchanged. Parameter B affects the rate of cumulative strain on the ε_P -N curve, which is mainly related to the properties of sand itself. Ren et al.[26] have found that the exponential parameter B should be a constant and has nothing to do with the load borne. As can be seen from Fig.10(c), when parameters A and B are determined, the ε_P -N curve basically shifts to the right with the increase of model parameter C, and the amount of translation gradually decreases. The model parameter C mainly determines the stabilization time of the ε_P -N curve. The larger the value of C is, the longer the stabilization time will be, but the final cumulative plastic strain and cumulative plastic strain rate remain unchanged.

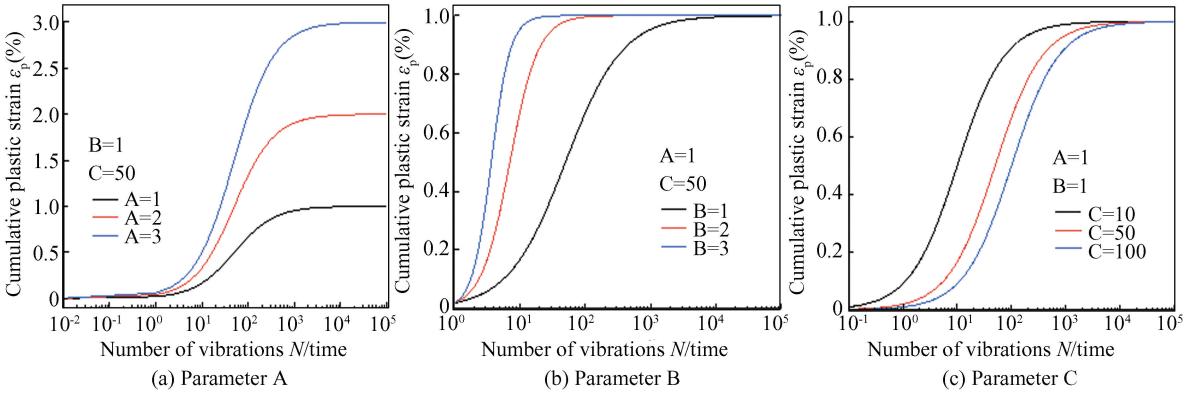

Fig.10 Effect of the model parameters on the cumulative plastic strain

3 Conclusions

In this paper, the effects of the number of reinforced layers, confining pressure and mesh size of geogrids on the cumulative plastic strain of reinforced sand under multi-stage cyclic loading are analyzed, and the corresponding cumulative plastic strain prediction model is improved. According to the analysis of the test results, the following conclusions are drawn:

(1) The relationship between the cumulative plastic strain and vibration times of the sample under different reinforcement layers shows three stages, the first stage is the rapid development stage of the cumulative plastic strain value. The second stage is the cumulative plastic strain rate transformation stage. The third stage is the stable stage.

(2) With the increase of the number of reinforced layers, the cumulative plastic strain of the sample gradually decreases, and the reinforcement can effectively improve the stiffness of the sample and reduce the settlement deformation of the sandy soil roadbed. However, with the increase of the number of reinforced layers, the influence of reinforcement on the cumulative plastic strain gradually decreases.

(3) The effect of increasing confining pressure and decreasing mesh size on cumulative plastic strain is similar to that of increasing the number of reinforced layers. The cumulative plastic strain of the sample can be significantly reduced by increasing the confining pressure, and the deformation resistance of the reinforced sand sample can be further enhanced when the mesh size is reduced.

(4) Among the models for predicting cumulative plastic strain, the hyperbolic model has the worst

fitting effect, and the Monismith model has the fitting coefficient R^2 higher than 0.97, while the comprehensive model in this paper has the highest fitting coefficient R^2 higher than 0.99, which can better predict the cumulative plastic strain of unreinforced sand and reinforced sand.

(5) The joint strength of the geogrid joints used in this paper is weak. It is suggested that the influence of geogrid joint strength on the strength properties of reinforced sand should be considered in future tests. It is suggested that dynamic triaxial test conditions should be added in the future, and the parameters of the comprehensive cumulative plastic strain model should be investigated using the test data. The relationship between each parameter and the test conditions will be obtained and a model related to the number of reinforced layers will be established.

References

[1] Wichtmann T, Triantafyllidis T. Stress attractors predicted by a high-cycle accumulation model confirmed by undrained cyclic triaxial tests. Soil Dynamics and Earthquake Engineering, 2015, 69(2): 125-137. DOI: 10.1016/j.soildyn.2014.10.013.

[2] Nguyen N S, François S, Degrande G. Discrete modeling of strain accumulation in granular soils under low amplitude cyclic loading. Computers and Geotechnics, 2014, 62: 232-243. DOI: 10.1016/j.compgeo.2014.07.015.

[3] Huang B, Ding H, Chen Y. Simulation of high-speed train load by dynamic triaxial tests. Journal of Geotechnical Engineering, 2011, 33(2): 195-202.

[4] Huang J, Wang H, Chen J, et al. Effects of intermittent cyclic loading with cyclic confining pressure on deformation behaviors of saturated clay. Chinese Journal of Geotechnical Engineering, 2023, 45(S1): 67-70. DOI: 10.11779/CJGE2023S10038.

[5] Wang J, Chang Z, Tang Y, et al. Dynamic triaxial test analysis of reinforced gravel soil under cyclic loading. Rock and Soil Mechanics, 2020, 41(9): 2851-2860. DOI: 10.16285/j.rsm.2019.1977.

[6] Song F, Chen W. Research on large-scale dynamic triaxial tests of geogrid reinforced sand. Journal of Railway Science and Engineering, 2022, 19(3): 683-690. DOI: 10.19713/j.cnki.43-1423/u.t20210247.

[7] Cui K, Zhang D, Li Q, et al. Experimental investigation on the accumulated strain of coarse-grained soil reinforced by geogrid under high-cycle cyclic loading. Geotextiles and Geomembranes, 2023, 51(1): 233-244. DOI:10.1016/J.GEOTEXMEM.2022.11.001.

[8] Monismith C L, Ogawa N, Freeme C R. Permanent deformation characteristics of subgrade soils due to repeated loading. 54th Annual Meeting of the Transportation Research Board. Washington: Transportation Research Board, 1975(537): 1-17. http://onlinepubs.trb.org/Onlinepubs/trr/1975/537/537-001.pdf.

[9] Lentz R W. Permanent Deformation of Cohesionless Subgrade Material Under Cyclic Loading. East Lansing: Michigan State University, 1979. 5-24. DOI: 10.25335/2ycs-9m94.

[10] Zhang Y, Kong L, Guo A, et al. Cumulative plastic strain of saturated soft clay under cyclic loading. Rock and Soil Mechanics, 2009, 30(6): 1542-1548. DOI: 10.16285/j.rsm.2009.06.012.

[11] Li D, Selig E T. Cumulative plastic deformation for fine-grained subgrade soils. Journal of Geotechnical Engineering, 1996, 122(12): 1006-1013. DOI: 10.1061/(ASCE)0733-9410(1996)122:12(1006).

[12] Chai J C, Miura N. Traffic-load-induced permanent deformation of road on soft subsoil. Journal of Geotechnical and Geoenvironmental Engineering, 2002, 128(11): 907-916. DOI: 10.1061/(ASCE)1090-0241(2002)128:11(907).

[13] Gao H, Dong D Zhao Q, et al. Study on dynamic response of reinforced soil subgrade under cyclic loading. Journal of Disaster Prevention and Mitigation Engineering, 2022, 42(1): 208-230. DOI: 10.13409/j.cnki.jdpme.201910031.

[14] Wang K. Study on dynamic response and cumulative settlement characteristics of foundation in transition section of heavy haul railway tunnel in Loess area. Beijing Jiaotong University, 2018, 184: 10-22.

[15] Liu B, Su Q, Pham D P, et al. Study of critical dynamic stress and deformation law of graded gravel under different moisture content. Journal of the China Railway Society, 2016, 38(6): 100-107. DOI: 10.3969/j.issn.1001-8360.2016.06.015.

[16] Li L, Qin L, Xiao H, et al. Large scale dynamic triaxial test and reinforcement mechanism exploration of reinforced construction waste soil. Journal of Rock Mechanics and Engineering, 2020, 39(8): 1682-1695. DOI: 10.13722/j.cnki.jrme.2019.1146.

[17] Chen Y, Bian X. Vibration and settlement caused by high-speed traffic. Proceedings of the 7th National Soil Dynamics Academic Conference, Beijing: Tsinghua University Press, 2006: 5-6. https://d.wanfangdata.com.cn/conference/ChZDb25mZXJlbmNlTmV3UzIwMjQwMTA5Egc2MjcxODA5GghiZHBpcG1qdw==.

[18] Erlingsson S, Rahman M S. Evaluation of permanent deformation characteristics of unbound granular materials by means of multi-stage repeated load triaxial test. Journal of the Transportation Research Board, 2013, 2369(1): 11-19. DOI: 10.3141/2369-02.

[19] Tang L, Yan M H, Ling X Z, et al. Dynamic behaviours of railway's base course materials subjected to long-term low-level cyclic loading: Experimental study and

empirical model. Géotechnique, 2017, 67(6):537-545. DOI: 10.1680/JGEOT.16.P.152.

[20] China Railway Eryuan Engineering Group Co., LTD. TB 10025 - 2019 Code for Design of Railway Subgrade Retaining Structure. Beijing: China Railway Publishing House, 2020.

[21] Ma S, Wang B, Liu Y, et al. Large-scale dynamic triaxial tests on saturated gravel soil in Nanning metro area. Chinese Journal of Geotechnical Engineering, 2019, 41(1):168-174. DOI: 10.11779/CJGE201901019.

[22] Wang J, Zhang L, Chen Y, et al. Discrete element microscopic analysis of geogrid reinforced sand triaxial test. Journal of Hydraulic Engineering, 2017, 48(4): 426-434. DOI:10.13243/j.cnki.slxb.20160829.

[23] Bao C. Application Principles and Engineering Practice of Geosynthetic Materials. Beijing: China Water Resources and Hydropower Publishing House, 2008, 129 - 130. ISBN:978-7-5084-5616-4.

[24] Li Y, Nie R, Li Yu, et al. Permanent deformation characteristics and prediction model of fine-grained soil fill in roadbed under intermittent cyclic loading. Rock and Soil Mechanics, 2021, 42(4): 1065 - 1077. DOI: 10.16285/j.rsm.2020.1210.

[25] Nie R, Xiao L, Tan Y, et al. Research on the rebound and cumulative plastic strain characteristics of coarse-grained soil fill under the load of beam transport vehicles. Journal of Railway Science and Engineering, 2023, 20(8): 2847-2857. DOI: 10.19713/j.cnki.43-1423/u.t20221760.

[26] Ren X, Xu Q, Teng J, et al. A novel model for the cumulative plastic strain of soft marine clay under long-term low cyclic loads. Ocean Engineering, 2018, 149(1): 194-204. DOI: 10.1016/j.oceaneng.2017.12.028.